

Transverse-momentum distribution of Higgs bosons at the Superconducting Super Collider

Ian Hinchliffe and S. F. Novaes

Lawrence Berkeley Laboratory, University of California, Berkeley, California 94720

(Received 13 June 1988)

We consider the transverse-momentum distribution of Higgs-boson production in gluon-gluon fusion. Using resummation techniques we obtain a result valid at all transverse momenta. The resulting distributions are compared with those from the WW fusion mechanism and with those produced by event generators.

The ability to detect the standard-model Higgs boson has become one of the benchmarks for high-energy hadron colliders. The Higgs boson is produced by two mechanisms: gluon + gluon $\rightarrow H$ via a virtual quark loop¹ and the so-called WW fusion² process quark + quark $\rightarrow H$ + quark + quark. The relative importance of these two mechanisms depends upon the Higgs-boson and top-quark masses. For a top quark of mass of order 40 GeV, the former dominates for Higgs-boson masses less than about 300 GeV. If the top mass is close to its maximum allowed value of 180 GeV, then the gluon-fusion process is dominant out to Higgs-boson masses of order 1 TeV (see Fig. 1).

At lowest order in QCD perturbation theory, the gluon-gluon-fusion process produces a Higgs boson with almost zero transverse momentum (p_\perp) (the intrinsic transverse momentum of the gluon in the proton is negligible). The WW fusion process, however, produces a Higgs boson with transverse momentum of order M_W ; the p_\perp is balanced by the recoiling quark pair. The distribution in transverse momentum is important when a strategy is devised to detect the Higgs boson. The main background in the decay channel $H \rightarrow ZZ \rightarrow 4l$, where l denotes either an electron or muon, arises from the process $q\bar{q} \rightarrow ZZ$ (Ref. 3). In the event of a detection system with poor resolution on the lepton-pair invariant mass, the process $gg \rightarrow Z + t\bar{t}$ followed by the semileptonic decay of both the top quark and antiquark can produce an additional "fake" Z . In the latter case the transverse momenta of the real and "fake" Z do not balance, and this mismatch may be used to reject this background if it is important.⁴ It has been suggested that, in the WW fusion case, the additional quark jets can be used as a tag to increase the background rejection.⁵

In this paper we will discuss the transverse-momentum distribution of the Higgs boson from the gluon-gluon process, will show that it is quite broad, and in particular that the average p_\perp is comparable to that from the WW fusion process for Higgs-boson masses of 500 GeV or more.

The process $gg \rightarrow H$ proceeds at order α_s^2 . A Higgs boson can be produced at large p_\perp from the processes $gg \rightarrow Hg$, $gq \rightarrow qH$, and $q\bar{q} \rightarrow Hg$ which occur at order α_s^3 . The first two processes are divergent as p_\perp tends to zero.⁶ In this region it is necessary to take into account multiple-gluon emission which generates terms of order

$$\frac{1}{p_\perp^2} \alpha_s^n \ln^m(M_H^2/p_\perp^2)$$

with $m \leq 2n - 3$. The largest of these terms, those in the double leading-log approximation ($m = 2n - 3$), can be resummed, as was originally done in the case of Drell-Yan production.⁷ The procedure has been extended to include terms which are less singular.⁸ For the purposes of studying a typical Higgs-boson event it is necessary to have a description of the p_\perp distributions which is valid at all p_\perp : that is, one which correctly reproduces the lowest-order result at large p_\perp and the resummed result at small p_\perp . A procedure for doing this has been given⁹ and applied to the production of W bosons at the CERN $Spp\bar{S}$ collider.¹⁰

The rest of this paper is organized as follows. We first derive the p_\perp distribution valid over all p_\perp . In doing this we shall simplify the task by assuming that the heaviest quark contributing to the loop is large. The formulas simplify enormously in this limit. The accuracy of the approximate formulas in the large- p_\perp region have been investigated in detail elsewhere.⁶ In practice the approximation is good to better than a factor of 3 or so if $m_q \gtrsim (M_H^2 + p_\perp^2)^{1/2}/4$. (See Figs. 5-7 of Ref. 6.) In this paper we are primarily interested in the shape of the dis-

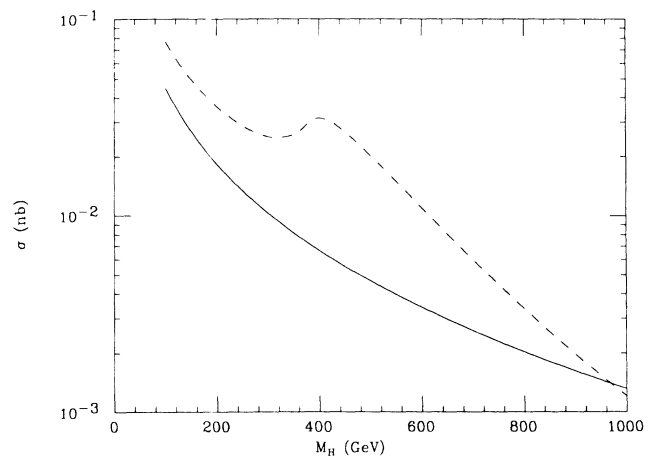


FIG. 1. The total cross section for the production of a Higgs boson at $\sqrt{s} = 40$ TeV. The solid line corresponds to the WW fusion process and the dashed (dotted) to the gluon-gluon fusion with $m_{\text{top}} = 180$ (50) GeV.

tribution, not its absolute normalization. We then present the p_1 distribution noting the severe numerical problems which arise in its computation. Finally, we compare the distribution with that arising from the WW fusion process,^{2,5} and also with that given by some popular event generators^{11,12} which are used for simulation events at the Superconducting Super Collider (SSC).

In the limit where the internal quark mass is large the process $gg \rightarrow gH$ which proceeds via an intermediate quark loop (see Fig. 2) has the differential cross section

$$\frac{d\sigma}{dt} = \frac{3A\alpha_s}{2\pi s^2} \left[\frac{s^4 + t^4 + u^4 + M_H^8}{stu} \right]. \quad (1)$$

Here s , t , and u are the usual Mandelstam variables and $A = \frac{1}{576}(\alpha_W \alpha^2 / M_W^2)$. This can be used to generate the p_1 distribution of the Higgs boson in the process $pp \rightarrow H + X$ using the usual parton model formula, viz.,

$$\begin{aligned} \frac{d\sigma}{dp_1^2 dy} &= \frac{1}{s} \int_{\sqrt{\tau^+ e^y}}^1 \frac{dx_1}{x_1 - x_1^+} G(x_1, Q^2) G(x_2^*, Q^2) \\ &\quad \times \hat{s} \frac{d\sigma}{d\hat{t}}(\hat{s}, \hat{t}, \hat{u}) \\ &+ \frac{1}{s} \int_{\sqrt{\tau^+ e^{-y}}}^1 \frac{dx_2}{x_2 - x_2^+} G(x_1^*, Q^2) G(x_2, Q^2) \\ &\quad \times \hat{s} \frac{d\sigma}{d\hat{t}}(\hat{s}, \hat{t}, \hat{u}). \end{aligned} \quad (2)$$

Here the following variables have been introduced; the incoming proton momenta are p_1 and p_2 and p_H is the momentum of the Higgs boson, which has rapidity y . Then

$$\begin{aligned} s &= (p_1 + p_2)^2, \quad t = (p_1 - p_H)^2, \quad u = (p_2 - p_H)^2, \\ \tau &= M_H^2/s, \quad \sqrt{\tau^+} = (p_1^2/s)^{1/2} + (\tau + p_1^2/s)^{1/2}, \\ x_1^+ &= (M_H^2 - u)/s, \quad x_2^+ = (M_H^2 - t)/s, \\ x_1^* &= (x_2 x_1^+ - \tau)/(x_2 - x_2^+), \\ x_2^* &= (x_1 x_2^+ - \tau)/(x_1 - x_1^+). \end{aligned}$$

$$\begin{aligned} \frac{d\sigma}{dp_1^2 dy} &= \frac{3A\alpha_s}{2\pi} \int_{\sqrt{\tau^+ e^y}}^1 \frac{dx_1}{x_1 - x_1^+} \frac{1}{p_1^2} \left\{ H(x_1, x_2^*) \frac{\hat{s}}{s} \left[1 + \left[1 - \frac{\tau}{x_1 x_2^*} \right]^4 + \left[\frac{\tau}{x_1 x_2^*} \right]^4 \right] - 2\tau H(x_1^0, x_2^0) \right\} \\ &+ \frac{3A\alpha_s}{\pi p_1^2} \int_{\sqrt{\tau^+ e^y}}^1 \frac{dx_1}{x_1 - x_1^+} \tau H(x_1^0, x_2^0) + \frac{3A\alpha_s}{2\pi s} \int_{\sqrt{\tau^+ e^y}}^1 \frac{dx_1}{x_1 - x_1^+} \left[\frac{2p_1^2}{\hat{s}} - 4 \left[1 - \frac{\tau}{x_1 x_2^*} \right]^2 \right] H(x_1, x_2^*). \end{aligned} \quad (4)$$

Here we have added and subtracted terms which are singular as $p_1 \rightarrow 0$, and have introduced the variables $x_1^0 = \sqrt{\tau} e^y$, $x_2^0 = \sqrt{\tau} e^{-y}$, and $H(x, y) \equiv G(x, Q^2) G(y, Q^2)$. The remaining singularities at $p_1 = 0$ are canceled by the virtual corrections to the lowest-order process $gg \rightarrow H$ which are of the form

$$\frac{d\sigma_2}{dp_1^2 dy} \sim A \left[\frac{\alpha_s}{2\pi} \right] \delta(p_1^2) H(x_1^0, x_2^0). \quad (5)$$

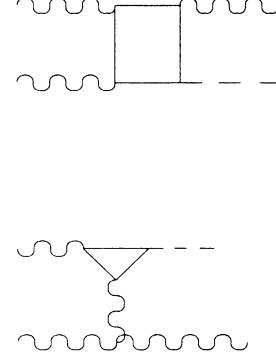


FIG. 2. Feynman diagrams showing contributions to the process $gg \rightarrow gH$.

The partonic cross section $\hat{s} d\sigma/d\hat{t}$ is evaluated at the momentum transfers appropriate to the subprocess, i.e., $\hat{s} = s x_1 x_2$, $\hat{t} = x_1(t - M_H^2) + M_H^2$, $\hat{u} = x_2(u - M_H^2) + M_H^2$.

In Eq. (2), $G(x, Q^2)$ is the distribution of gluons in the proton. The scale Q^2 appearing in the gluon distribution and in α_s is ambiguous. The sensitivity to this ambiguity can only be reduced by investigation of order- α_s^4 effects. Provided that this formula is used in the region $p_1 \sim M_H$, the results obtained by using the choices $Q = M_H$ or $Q = p_1$ will not be too different. We shall return to this issue below.

The modifications to Eq. (2) in order to make it valid over all p_1 are as follows.^{8,9} We must break it into two pieces, one of which is singular as $p_1 \rightarrow 0$, the other of which is not. First, write the partonic cross section Eq. (1) as

$$\hat{s} \frac{d\sigma}{dt} = 3A \left[\frac{\alpha_s}{2\pi} \right] \left\{ \frac{\hat{s}}{p_1^2} \left[\left[1 - \frac{\tau}{x_1 x_2} \right]^4 + 1 + \left[\frac{\tau}{x_1 x_2} \right]^4 \right] - 4 \left[1 - \frac{\tau}{x_1 x_2} \right]^2 + \frac{2p_1^2}{\hat{s}} \right\}. \quad (3)$$

The x_1 integral of Eq. (2) may now be rewritten as

After integration over p_1 , we obtain the total Higgs-boson production rate to order α_s^3 . In view of this we can regulate the singularities in Eq. (4) by replacing $1/p_1^2$ by $(1/p_1^2)_+$, where the (+) is defined so that

$$\int_0^{p_{\max}} \frac{dp_1^2 f(p_1^2)}{(p_1^2)_+} = \int_0^{p_{\max}} \left[\frac{f(p_1^2) - f(0)}{p_1^2} \right] dp_1^2. \quad (6)$$

The upper limit of the p_1 integration (p_{\max}) in these distributions can be taken to be either M_H or the maximum

allowed p_1 . We will choose the former so as to avoid terms proportional to $\ln(p_{1\max}/M_H)$ which can be large.

We have not computed the virtual contributions and will not therefore include them in what follows. This omission means that the integral over p_1 of our final result, although of order α_s^3 , does not reproduce the full order- α_s^3 rate. However, this is not important since we are interested only in the shape of the distribution. Furthermore, the mean value of p_1^2 is given correctly at order α_s without the inclusion of these virtual corrections.

We now add and subtract the term

$$\frac{A\alpha_s}{2\pi} \int_{x_1^0}^1 \frac{dz}{z} P_{gg}(z) H(x_1^0/z, x_2^0) \quad (7)$$

from Eq. (4). Here $P_{gg}(z)$ is the Altarelli-Parisi splitting functions¹³

$$P_{gg}(z) = 6 \left[\frac{1-z}{z} + \left(\frac{z}{1-z} \right)_+ + z(1-z) \right] + \kappa\delta(1-z), \quad (8)$$

where $\kappa = \frac{11}{2} - n_f/3$ and n_f is the number of light flavors. Following this manipulation (and adding the x_2 integral), we get

$$\frac{d\sigma}{dp_1^2 dy} = X + Y, \quad (9)$$

where

$$X_g = \frac{3A\alpha_s\tau}{\pi} \left[\frac{1}{p_1^2} \ln(M_H^2/p_1^2) - \frac{\kappa}{3p_1^2} \right] H(x_1^0, x_2^0) + \frac{A\tau}{p_1^2} \left[\frac{\alpha_s}{2\pi} \right] \left[\int_{x_1^0}^1 \frac{dz}{z} P_{gg}(z) H(x_1^0/z, x_2^0) + (1 \leftrightarrow 2) \right] \quad (10)$$

and

$$\begin{aligned} Y_1 &= \frac{3A\alpha_s}{2\pi s} \left\{ \int_{\sqrt{\tau^+} e^y}^1 \frac{dx_1}{x_1 - x_1^+} \left[\frac{2p_1^2}{\hat{s}} - 4 \left[1 - \frac{\tau}{x_1 x_2^*} \right]^2 \right] H(x_1, x_2^*) + (1 \leftrightarrow 2) \right\}, \\ Y_2 &= \frac{3A\alpha_s}{2\pi} \frac{1}{p_1^2} \left\{ \int_{\sqrt{\tau^+} e^y}^1 \frac{dx_1}{x_1 - x_1^+} \left[H(x_1, x_2^*) \frac{\hat{s}}{s} \left[1 + \left[1 - \frac{\tau}{x_1 x_2^*} \right]^4 + \left[\frac{\tau}{x_1 x_2^*} \right]^4 \right] - 2H(x_1^0, x_2^0) \tau \right] + (1 \leftrightarrow 2) \right\}, \\ Y_3 &= -\frac{3A\alpha_s}{2\pi} \frac{1}{p_1^2} \left\{ \int_{x_1^0}^1 \frac{dx_1}{x_1 - x_1^0} \left[\tau H(x_1, x_2^0) \frac{x_1}{x_1^0} \left[1 + \left[1 - \frac{x_1^0}{x_1} \right]^4 + \left[\frac{x_1^0}{x_1} \right]^4 \right] - 2\tau H(x_1^0, x_2^0) \right] + (1 \leftrightarrow 2) \right\}, \\ Y_4 &= \frac{3A\alpha_s}{\pi} \frac{\tau}{p_1^2} H(x_1^0, x_2^0) \ln \left[\frac{(1-x_1^+)(1-x_2^+)}{(1-x_1^0)(1-x_2^0)} \right]. \end{aligned} \quad (11)$$

Note that $Y = Y_1 + Y_2 + Y_3 + Y_4$ is finite as $p_1 \rightarrow 0$. Before proceeding further it is necessary to include the terms from the process $gq \rightarrow Hq$ for which the partonic cross section in the large-fermion-mass limit is⁶

$$s \frac{d\sigma}{dt} = -\frac{4A}{3} \frac{\alpha_s}{2\pi} \frac{1}{p_1^2} \left[\frac{u^3 + us^2}{s^2} \right]. \quad (12)$$

Following manipulations similar to those above,

$$\frac{d\sigma}{dp_1^2 dy} = X_q + Y_q, \quad (13)$$

$$\begin{aligned} Y_q &= -\frac{4A}{3p_1^2} \left[\frac{\alpha_s}{2\pi} \right] \left\{ \int_{-u/(s+t-M_H^2)}^1 \frac{dx_1}{x_1 s + u - M_H^2} q(x_1) G(x_2^q) \left[\frac{\hat{t}^3}{\hat{s}^2} + \hat{t} \right] \right. \\ &\quad + \int_{-t/(s+u-M_H^2)}^1 \frac{dx_2}{x_2 s + t - M_H^2} q(x_2) G(x_1^q) \left[\frac{\hat{u}^3}{\hat{s}^2} + \hat{u} \right] \\ &\quad \left. + \tau G(x_1^0) \int_{x_2^0}^1 \frac{dx_2}{x_2^0} q(x_2) [1 + (1-x_2^0/x_2)^2] + \tau G(x_2^0) \int_{x_1^0}^1 \frac{dx_1}{x_1^0} q(x_1) [1 + (1-x_1^0/x_1)^2] \right\}, \quad (14) \end{aligned}$$

$$X_q = \frac{A\tau}{p_1^2} \left[\frac{\alpha_s}{2\pi} \right] \left[G(x_1^0) \int_{x_2^0}^1 \frac{dz}{z} P_{gq}(z) q(x_2^0/z) + (1 \leftrightarrow 2) \right],$$

where

$$x_1^q = [-x_2 u - M_H^2(1-x_2)] / (x_2 s + t - M_H^2),$$

$$x_2^q = [-x_1 t - M_H^2(1-x_1)] / (x_1 s + u - M_H^2),$$

and

$$P_{gq}(x) = \frac{4}{3} \frac{1+(1-x)^2}{x}.$$

The final contribution from the process $q\bar{q} \rightarrow Hg$ is finite⁶ as $p_\perp \rightarrow 0$. It is small numerically, contributes to Y only, and is not written explicitly.

We now have

$$\frac{d\sigma}{dp_\perp^2 dy} = X_q + X_g + Y_1 + Y_2 + Y_3 + Y_4 + Y_q. \tag{15}$$

We now perform the resummation on the term $X = X_q + X_g$. Perform a Fourier transform

$$X(p_\perp) = \int \frac{d^2b}{4\pi} e^{-ib \cdot p_\perp} X(b). \tag{16}$$

We have

$$X(b) = A\tau H(x_1^0, x_2^0) \left[1 + \frac{3\alpha_s}{\pi} \int_0^{p_{\max}} \frac{dp^2}{p^2} [J_0(bp) - 1] \left[\ln(M_H^2/p^2) - \frac{\kappa}{3} \right] \right] \\ + A\tau \frac{\alpha_s}{2\pi} \ln(M_H^2 b^2) \left[\int_{x_1^0}^1 \frac{dz}{z} P_{gg}(z) H(x_1^0/z, x_2^0) + \int_{x_1^0}^1 \frac{dz}{z} P_{gq}(z) q(x_1^0/z) G(x_2^0) + (1 \leftrightarrow 2) \right]. \tag{17}$$

Here $J_0(x)$ is a Bessel function. Had we included the virtual (order- α_s^3) terms, there would be further terms in the equation proportional to $A\alpha_s$ but independent of b . The structure functions appearing in Eq. (17) are to be evaluated at $Q^2 \simeq m_H^2$. Notice that the solution of the Altarelli-Parisi equations is

$$G(x, 1/b^2) = G(x, Q^2) + \frac{\alpha_s}{2\pi} \ln(Q^2 b^2) \left[\int_x^1 \frac{dz}{z} P_{gg}(z) G(x/z, Q^2) + \int_x^1 \frac{dz}{z} P_{gq}(z) q(x/z, Q^2) \right] + O(\alpha_s^2). \tag{18}$$

Hence, we may rewrite

$$X(b) = A\tau H(x_1^0, x_2^0, 1/b^2) \left[1 + \frac{3\alpha_s}{\pi} \int \frac{dp^2}{p^2} [J_0(bp) - 1] [\ln(M_H^2/p^2) - \kappa/3] \right]. \tag{19}$$

The resummation of the dominant terms at small p_\perp leads to^{7,8}

$$X(b) \rightarrow A\tau H(x_1^0, x_2^0, 1/b^2) e^{S(b)}, \tag{20}$$

where

$$S(b) = \frac{3\alpha_s}{\pi} \int_0^{M_H^2} \frac{dp^2}{p^2} [J_0(bp) - 1] [\ln(M_H^2/p^2) - \kappa/3].$$

The full result is then

$$\frac{d\sigma}{dp_\perp^2 dy} = Y_1 + Y_2 + Y_3 + Y_4 + Y_q \\ + A\tau \int \frac{d^2b}{4\pi} e^{-i(b \cdot p_\perp)} H(x_1^0, x_2^0) e^{S(b)}. \tag{21}$$

The process $q\bar{q} \rightarrow Hg$ (Ref. 6) is finite as $p_\perp \rightarrow 0$ and, hence, needs no resumming, and can be added to Eq. (21). Numerically it is insignificant, but we have included it in the values shown in the figures. Equation (21) can now be evaluated numerically to obtain a distribution which is valid at all p_\perp . At small values, the terms in Y are negligible and those of X alone control the distribution. At large p_\perp there is a very delicate cancellation between X and Y in order to recover the lowest-order result. In order to understand this, notice that the dominant term in Y is Y_3 , since the structure functions fall rapidly with x and it has the lowest lower limit in the integrals over x_1

and x_2 . This produces a term proportional to $1/p_\perp^2$ since there is no p_\perp dependence in the integrals. The full lowest-order result falls much more rapidly since $\sqrt{\tau^+} e^\nu$ which in the lower limit on the integral in Eq. (2) increases with p_\perp .

This dominant term is canceled by appropriate terms in X . Notice that this cancellation involves the term of Eq. (17) which is an approximate solution (18) to the Altarelli-Parisi equations for the evolution of structure functions. Since X is evaluated using a set of structure functions which are obtained by an exact solution, small differences will arise which destroy the cancellation. The main difference is that (18) is a solution to the Altarelli-Parisi equations assuming the α_s is a constant. The full solution to

$$\frac{d}{d \ln Q^2} G(x, Q^2) = \frac{\alpha_s(Q^2)}{2\pi} \int_x^1 \frac{dz}{z} [G(x/z, Q^2) P_{gg}(z) \\ + q(x/z, Q^2) P_{gq}(z)] \tag{22}$$

will differ slightly.

The numerical values for the structure functions also need to be much more accurate than the few percent normal in a parametrization. The difficulty caused by the nature of this extremely delicate cancellation can be seen

in Fig. 3 where the result of Eq. (21) is compared to the order- α_s^3 result $m_H=200$ GeV. There is a region of p_\perp where the curves come together, and a region at larger p_\perp where the numerical cancellation fails and the evaluation of Eq. (21) fails to reproduce the lowest-order result. In obtaining Fig. 3 Eichten-Hinchliffe-Lane-Quigg (EHLQ) set-2 (Ref. 14) structure functions were used. The $\alpha_s(\mu)$ appearing in A was evaluated at $\mu^2=M_H^2$, while that appearing explicitly in $S(b)$ was evaluated at $\mu^2=1/b^2$ and that in Y at $\mu^2=p_\perp^2$. This choice, although arbitrary, is a reasonable one. Calculation to order α_s^4 are needed in order to reduce the ambiguities inherent in these choices.

In order to circumvent the numerical problem, we adopt the following prescription. Choose a value of $p_\perp=p_\perp^0$ where the two curves in Fig. 3 overlap. Then define

$$\frac{d\sigma}{dp_\perp^2 dy} = \left[1 - f \left(\frac{p_\perp}{p_\perp^0} \right) \right] [\text{Eq. (21)}] + f \left(\frac{p_\perp}{p_\perp^0} \right) (\text{lowest order}), \quad (23)$$

where $f(1)=0.5$ and $f(x)$ goes rapidly to zero (one) as x falls below (rises above) the point $x=1$. There is little sensitivity to p_\perp^0 provided that it is chosen in this way. Notice that the value of p_\perp^0 is different for each value of M_H ; the choice $p_\perp^0=M_H/3$ works well.

It is worth remarking that similar problems can afflict applications of the same technique to computation of the p_\perp distribution of W and Z bosons at the $Sp\bar{p}S$ and Fermilab Tevatron colliders. Here the numerical cancellations are difficult for $p_\perp > 20$ GeV and the above prescription should be adopted in this case also.

Figure 4 shows the p_\perp distributions of Higgs bosons on mass 100, 200, 400, and 800 GeV. From these figures we can determine the average p_\perp :

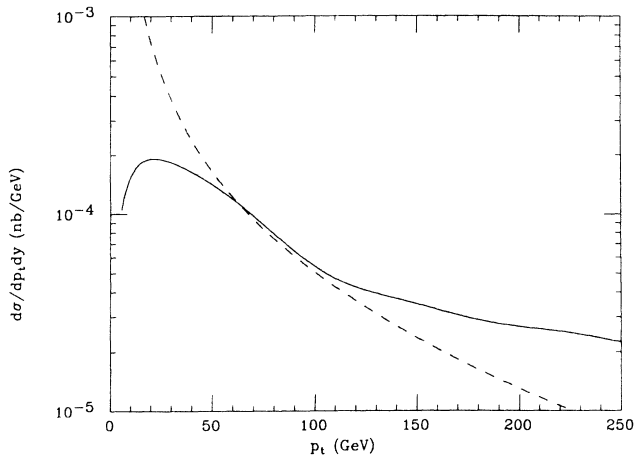


FIG. 3. The cross section $d\sigma/dp_\perp dy$ for the production of a Higgs boson from the gluon-gluon process at $y=0$ for $m_H=200$ GeV and $\sqrt{s}=40$ TeV. The solid line corresponds to the resummed result of Eq. (21); the dashed to the lowest-order result. The failure of the curves to agree at large p_\perp is discussed in the text.

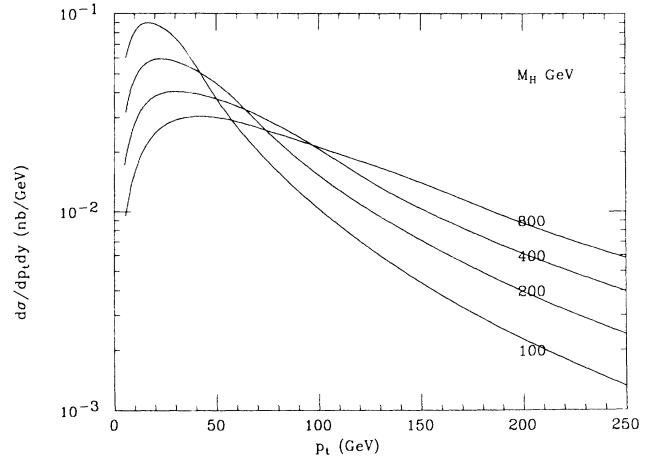


FIG. 4. The cross section $d\sigma/dp_\perp dy$ at $y=0$ for the process $pp \rightarrow H+X$ at $\sqrt{s}=40$ TeV for $m_H=100, 200, 400, 800$ GeV.

$$\langle p_\perp \rangle \sim [60 + 0.12(M_H - 100)] \text{ GeV} \quad (24)$$

with m_H in GeV. This average (60 GeV) is larger for a 100-GeV Higgs boson than that for the production of a Z at SSC (35 GeV). This larger value is due to the different production mechanisms. The Z is produced by $q\bar{q}$ and the H by gg annihilation. The gluon has a larger color charge than the quark and so radiates more gluons, which generate the nonzero p_\perp , than do the quarks.

For comparison we show in Fig. 5 the p_\perp distribution from the WW fusion process. Here the p_\perp is balanced by the outgoing quarks. The characteristic scale for this process is M_W , since the internal W have invariant mass of this order. Hence, the p_\perp of the Higgs boson is of order M_W and does not grow appreciably as the Higgs-boson mass is increased. There will be an additional contribution to this p_\perp due to the radiation of gluons off the incoming quarks, but this will not be large since the

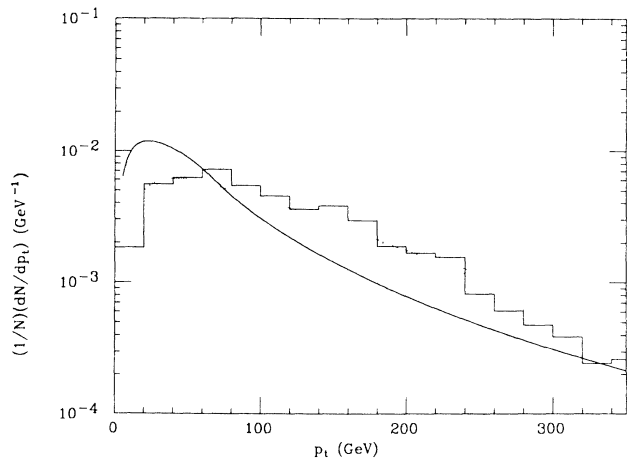


FIG. 5. A comparison of the distributions $d\sigma/dp_\perp dy$ at $y=0$ for Higgs-boson production at the SSC from the WW (histogram) and gluon-fusion (lines) processes. The solid (dotted) curves are for $M_H=200$ (800) GeV. The curves are normalized to the same area.

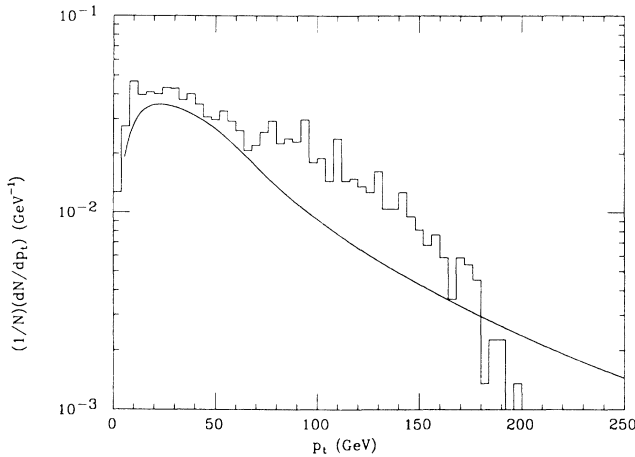


FIG. 6. A comparison of the p_{\perp} distribution $(1/N)dN/dp_{\perp}$ at $y=0$ for $m_H=200$ GeV. The histogram is the result of the ISAJET (Ref. 11) Monte Carlo simulation. The solid line is our result. The curves are normalized to the same area. The distribution for PYTHIA (Ref. 12) is similar to that of ISAJET.

quark color charge is smaller than that of the gluon and the characteristic scale of the process is m_W as opposed to M_H in the gluon-gluon case.

Finally, we would like to compare the p_{\perp} distribution that we have obtained with that produced by the event

generators PYTHIA (Ref. 12) and ISAJET (Ref. 11) which are often used to simulate events for SSC studies. These generators incorporate the process $gg \rightarrow H$ and allow the incoming gluons to radiate other gluons (initial-state radiation). It is this radiation which is responsible for the Q^2 dependence of the structure functions, and it also generates a nonzero p_{\perp} . This will be an approximation to the true p_{\perp} distribution discussed above. The partonic process $gq \rightarrow Hg$ and $q\bar{q} \rightarrow gH$ and $gg \rightarrow gH$ are not included explicitly in the generators. It can be seen from Fig. 6 the p_{\perp} distribution obtained by us has a different shape from that given by these Monte Carlo generators. However, the average p_{\perp} is very similar. It is clear that the distributions given by these event generations are probably adequate for signal/background studies. In conclusion, we have investigated the p_{\perp} distribution of the Higgs boson from the gluon-fusion process and have shown that the average value of p_{\perp} is quite large.

This work was supported by the Director, Office of Energy Research, Office of High Energy Physics, Division of High Energy Physics of the U.S. Department of Energy under Contract No. DE-AC03-76SF00098. One of us (S.F.N.) would like to thank the Theoretical Physics Group of the Lawrence Berkeley Laboratory for its kind hospitality and the Conselho Nacional de Desenvolvimento Científico e Tecnológico, Brazil for financial support.

- ¹H. M. Georgi, S. L. Glashow, M. E. Machacek, and D. V. Nanopoulos, *Phys. Rev. Lett.* **40**, 692 (1978).
²R. N. Cahn and S. Dawson, *Phys. Lett.* **136B**, 196 (1984); D. R. T. Jones and S. I. Petcov, *ibid.* **84B**, 440 (1979).
³For a review, see R. N. Cahn *et al.*, in *Proceedings of the 1987 Berkeley Workshop on Detectors and Experimental Areas at SSC*, edited by M. Gilchriese (World Scientific, Singapore, 1988).
⁴I. Hinchliffe and E. Wang (in preparation).
⁵R. N. Cahn, S. D. Ellis, R. Kleiss, and W. J. Stirling, *Phys. Rev. D* **35**, 1626 (1987); R. Kleiss and W. J. Stirling, *Phys. Lett. B* **200**, 193 (1987).
⁶R. K. Ellis, I. Hinchliffe, M. Soldate, and J. J. van der Bij, *Nucl. Phys.* **B297**, 221 (1988).
⁷Yu. L. Dokshitzer, D. I. Dyakanov, and S. I. Troyan, *Phys. Lett.* **78B**, 290 (1978); *Phys. Rep.* **58**, 269 (1980); G. Parisi and R. Petronzio, *Nucl. Phys.* **B154**, 427 (1979); G. Curci, M. Greco, and Y. Srivastava, *Phys. Rev. Lett.* **43**, 834 (1979);

Nucl. Phys. **B159**, 451 (1982).

- ⁸J. C. Collins and D. E. Soper, *Nucl. Phys.* **B193**, 381 (1981); **B194**, 445 (1982).
⁹S.-C. Chao, D. E. Soper, and J. C. Collins, *Nucl. Phys.* **B214**, 513 (1983).
¹⁰G. Altarelli, R. K. Ellis, M. Greco, and G. Martinelli, *Nucl. Phys.* **B246**, 12 (1984).
¹¹ISAJET, F. Paige and S. Protopopescu, in *Physics of the Superconducting Super Collider, Snowmass, 1986*, proceedings of the Summer Study, Snowmass, Colorado, 1986, edited by R. Donaldson and J. Marx (Division of Particles and Fields of the APS, New York, 1987).
¹²H.-U. Bengtsson and T. Sjostrand, *Comput. Phys. Commun.* **46**, 43 (1987).
¹³G. Altarelli and G. Parisi, *Nucl. Phys.* **B126**, 298 (1977).
¹⁴E. Eichten, I. Hinchliffe, K. Lane, and C. Quigg, *Rev. Mod. Phys.* **56**, 579 (1984).